World Academy of Science, Engineering and Technology
International Journal of Mechanical and Mechatronics Engineering
Vol:5, No:12, 2011

Transient Hydrodynamic and Thermal Behaviors of Fluid Flow in a Vertical Porous Microchannel under the Effect of Hyperbolic Heat Conduction Model

A. F. Khadrawi

Abstract**—**The transient hydrodynamics and thermal behaviors of fluid flow in open-ended vertical parallel-plate porous microchannel are investigated semi-analytically under the effect of the hyperbolic heat conduction model. The model that combines both the continuum approach and the possibility of slip at the boundary is adopted in the study. The Effects of Knudsen number Kn, Darcy number Da, and thermal relaxation time τ on the microchannel hydrodynamics and thermal behaviors are investigated using the hyperbolic heat conduction models. It is found that as Kn increases the slip in the hydrodynamic and thermal boundary condition increases. This slip in the hydrodynamic boundary condition increases as Da increases. Also, the slip in the thermal boundary condition increases as τ decreases especially the early stage of time.

Keywords**—**free convection, hyperbolic heat conduction, macroscopic heat conduction models in microchannel, porous media, vertical microchannel, microchannel thermal, hydrodynamic behavior.

I. Introduction

THE hydrodynamic and thermal behavior of fluid flow through a microchannel have been given great interest in recent research activities. The importance of the microchannel fluid flow arises from new applications in microelectromechanical devices, such as micropumps, microturbines, and microrobotics, and in electronic equipment cooling.The research works of momentum and heat transport behaviors in microdomain is the fundamental for developing these new techniques, and is also a foreground in the heat transfer field. The developing microscale thermal and fluidic systems typically have characteristic length of the order of 1–100 μm and often operate in gaseous environments at standard conditions, where the molecular mean free path is in the order of 100 nm. For these cases, the Knudsen number (Kn) , which is defined as the ratio of the mean free path of gas molecules to the characteristic dimension of channel, is in the range from 10^{-3} to, 10^{-1} namely the velocity-slip and temperature-jump regime. Therefore, the microscale thermal and fluidic system must take into account the effects of slip flow and temperature jump at wall. Several factors that are dominant in the microscale have been identified through a number of experimental, analytical, and numerical works. The approximations for continuum flow analysis fail for microscale flows as the characteristic length of the flow gradients (L) approaches the average distance traveled by molecules between collisions (mean free path, λ). The ratio of these quantities is known as the Knudsen number ($\mathrm{Kn} = \lambda/\mathrm{L}$) and is used to indicate the degree of flow rarefaction or scale of the flow problem. Rarefaction or microscale effects are ignored by the Navier-Stokes equations, and these equations are therefore strictly accurate only at a vanishingly small Kn (Kn < 0.001). The appropriate flow and heat transfer models depend on the range of the Kn, and a classification of the different gas flow regimes is as follows: Kn < 0.001 for continuum flow, 0.001 < Kn < 0.1 for slip flow, 0.1 < Kn <10 for transition flow, and 10 < Kn for free molecular flow [1]. In this study, the slip flow regime (0.001 < Kn < 0.1) is considered, in order to study the hydrodynamic and thermal behaviors of transient free-convection slip fluid flow in a vertical open ended microchannel filled with a porous medium using the hyperbolic heat conduction model under thermal equilibrium assumption between liquid and solid phases.

Thermal behavior of microchannels has been extensively investigated by many researchers using different models, design, geometrical and operating parameters. Most of these studies are based on the parabolic (diffusion) heat conduction model. The parabolic heat conduction model is able to describe the thermal behavior of these microchannels in many practical applications. However, there are numerous cases in which the utilization of the hyperbolic heat conduction model becomes essential [2]. Examples of these cases are very fast transient heat conduction processes, heat conduction at cryogenic temperatures, high heating rate processes and situations involve high temperature gradients similar to heat found in micro-systems. In these applications, lagging is expected to occur between the heat flux and the temperature gradient across the fluid domain. Cattaneo and Vernotte [3,4] suggested independently a modified heat flux model in the form:

$$\vec{q}(t+\bar{\tau},\vec{r}) - k\vec{\nabla}T(t,\vec{r}) \quad (1)$$

where $\vec{q}$ is the heat flux vector, k is the thermal conductivity and $\bar{\tau}$ is the phase-lag in the heat flux vector. The constitution law of Eq. (1) assumes that the heat flux vector (the effect) and the temperature gradient (the cause) across a material volume occur at different instants of time and the time delay between the heat flux and the temperature gradient is the relaxation time $\bar{\tau}$. The analyses of laminar heat transfer in slip-flow regime were first undertaken by [5-6] for tubes with uniform heat flux and a parallel plate channel or a circular tube with uniform wall temperature using continuum theory

A. F. Khadrawi is with Mechanical Engineering Department, Al-Balqa' Applied University, Al-Huson collage P.O. Box 50, Irbid 21510, Jordan. khadrawi99@yahoo.com

subject to slip-velocity and temperature-jump boundary conditions. The slip flow problem in microtubes has been widely conducted by investigators [7]. However, slip flow in microchannels has not been conducted as much as the slip flow in microtubes. Since the slip flow in microchannels requires a two-dimensional approach, its solution is relatively difficult compared to that of the slip flow in microtubes. Some of the slip flow studies in microchannels are summarized here. Yu and Ameel [8] studied slip flow heat transfer in microchannels and found that heat transfer increases, decreases, or remains unchanged, compared to non-slip flow conditions, depending on two dimensionless variables that include effects of rarefaction and the fluid/wall interaction. Then, there has been an enormous interest in research works of micro-system over the last decade [9-15]

The objective of this study is to investigate the porous microchannel transient behaviors using the hyperbolic heat conduction model under local thermal equilibrium assumption between the fluid and solid phases. The model that combines the continuum approach with slip at the boundaries is adopted in this investigation. In this study Darcy-Brinkman model is adopted to describe the fluid flow hydrodynamic and thermal behavior. The tangential velocities and stresses are assumed to be matched at the clear fluid/porous domains interface. The inclusion of the Brinkman term is justified when the porosity is high, i.e., $\varepsilon > 0.6$ [16]. The continuity of the tangential velocities and shear stresses at the interface is widely used in the literature. It is also believed that this approach gives good predictions especially when the porosity is high, i.e., $\varepsilon > 0.6$. It is worth mentioning here that Darcy-Brinkman model is adopted to describe the fluid flow hydrodynamics behavior. The microscopic Forchheimer inertial is neglected and this is justified in natural convection problems especially at small Rayleigh numbers. Effects of Knudsen number Kn, Darcy number Da, acceleration coefficient tensor Ca, and thermal relaxation time τ on the porous microchannel hydrodynamics and thermal behaviors are investigated using the hyperbolic heat conduction models.

II. Analysis

Consider transient laminar fully developed free convection fluid flow inside an open-ended vertical parallel-plate microchannel filled with porous media. The fluid and solid phases will be assumed to be in local thermal equilibrium. The porous medium is assumed to be homogeneous and isotropic. The fluid is assumed to be Newtonian with uniform properties. Also, it is assumed that both viscous dissipation and internal heat generation are absent. Referring to Fig. 1 and using the dimensionless parameters given in the nomenclature, the governing equations of the hydrodynamic and thermal behaviors, as described by the hyperbolic heat conduction model, are given as [17]:

$$\mathrm{C_a}\frac{\partial \mathrm{U}}{\partial \eta} = \frac{\partial^2 \mathrm{U}}{\partial \eta^2} - \frac{\mathrm{U}}{\mathrm{D_a}} + \theta, \tag{2}$$

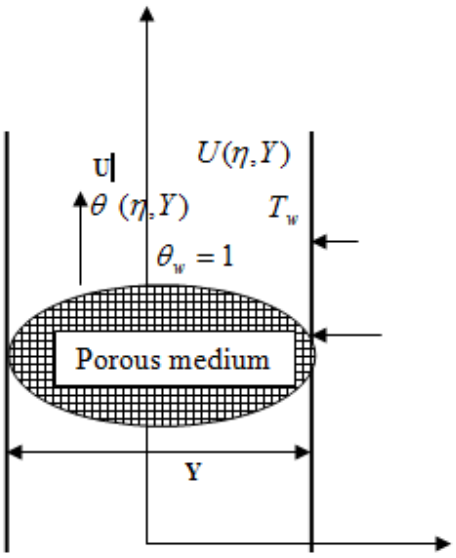

Fig. 1 schematic diagram of the problem under consideration

$$C_a\frac{\partial \theta}{\partial \eta} = -\frac{1}{Pr}\frac{\partial Q}{\partial Y} \tag{3}$$

$$Q + \tau\frac{\partial Q}{\partial \eta} = -\frac{\partial \theta}{\partial Y} \tag{4}$$

Equations (2-4) assume the following initial and boundary thermal conditions:

$$\theta(0,\tau) = \mathrm{U}(0,\mathrm{Y}) = 0, \tag{5}$$

$$\mathrm{U}(\eta,1) = -\Omega\ \mathrm{Kn}\ \frac{\partial \mathrm{U}(\eta,1)}{\partial \mathrm{Y}}, \tag{6}$$

$$\frac{\partial \mathrm{U}(\eta,0)}{\partial \mathrm{Y}} = 0,\ \frac{\partial \theta(\eta,0)}{\partial \mathrm{Y}} = 0\,, \tag{7}$$

$$\theta(\eta,1) - 1 = \mathrm{Kn}\ \frac{\psi}{\mathrm{Pr}}\mathrm{Q}(\eta,1), \tag{8}$$

where, $\Omega = (2-\sigma_v)/\sigma_v$, $\psi = (2-\sigma_T)(2\gamma)/(\sigma_T(\gamma+1))$, and $Kn = \lambda/L$. Also, the dimensionless slip-flow and temperature-jump boundary conditions are given as, respectively:

$$\Delta\mathrm{U}|_{\mathrm{wall}} = \mathrm{U}(\eta,1) = -\Omega\mathrm{Kn}\frac{\partial \mathrm{U}(\eta,1)}{\partial \mathrm{Y}}, \tag{8}$$

$$\Delta\theta|_{\mathrm{wall}} = \theta(\eta,1) - 1 = \mathrm{Kn}\frac{\psi}{\mathrm{Pr}}\mathrm{Q}(\eta,1), \tag{9}$$

where the right hand side of Eqs. (6) and (8) represents the slip in the hydrodynamic and thermal boundary condition of the boundary.

Equations (2-9) are solved using Laplace transformation technique. Now with the notation that $L\{\theta(\eta,Y)\} = W(S,Y), L\{Q(\eta,Y)\} = V(S,Y)$, and $L\{U(\eta,Y)\} = F(S,Y)$, Laplace transformation of Eqs. (2-9) yields:

$$\mathrm{C_a SF} = \frac{\mathrm{d^2F}}{\mathrm{d^2Y}} - \frac{\mathrm{F}}{\mathrm{D_a}} + \mathrm{W}, \tag{10}$$

$$SW = -\frac{1}{Pr}\frac{dV}{dY}, \quad (11)$$

$$V + \tau SV = -\frac{dW}{dY}, \quad (12)$$

Also, the Laplace transformation of the boundary conditions is given as:

$$\frac{\partial F(S,0)}{\partial Y} = 0, \quad (13)$$

$$F(S,1) = -\Omega Kn\frac{\partial F(S,1)}{\partial Y}, \quad (14)$$

$$\frac{\partial W(S,0)}{\partial Y} = 0, \quad (15)$$

$$W(S,1) - \frac{1}{S} = Kn\frac{\psi}{Pr}V(S,1) \quad (16)$$

According to the boundary conditions given in Eq. (16), Eqs. (13-15) are solved to give:

$$W = \frac{-C}{SPr}\beta\cosh(\beta Y), \quad (17)$$

$$V = C\sinh(\beta Y), \quad (18)$$

$$F = C_1\cosh(\sqrt{A}Y) + C_2\cosh(\beta Y), \quad (19)$$

$$\text{Where, } A = \left(C_a S + \frac{1}{D_a}\right),\ \beta = \sqrt{SPr(1+\tau S)}, \quad (20)$$

$$C = \frac{-1/S}{\frac{\beta}{SPr}\cosh(\beta) + Kn\frac{\psi}{Pr}\sinh(\beta)}, \quad (21)$$

$$C_1 = \frac{-C_2(\cosh(\beta) + \Omega Kn\beta\sinh(\beta))}{\cosh(\sqrt{A}) + \Omega Kn\sqrt{A}\sinh(\sqrt{A})}, \quad (22)$$

and,

$$C_2 = \frac{C\beta}{SPr(\beta^2 - A)} \quad (23)$$

Equations (17-19) are inverted in terms of Riemann-sum approximation [2] as:

$$\theta(\eta, Y) \approx \frac{e^{\xi\eta}}{\eta}\left(\frac{1}{2}W(\xi, Y) + Re\sum_{n=1}^{N} W\left(\xi + \frac{in\pi}{\eta}, Y\right)(-1)^n\right), \quad (24)$$

where Re refers to the "real part of" and $i = \sqrt{-1}$ is the imaginary number, *N* is the number of terms used in Riemann-sum approximation and ξ is the real part of the Bromwich contour that is used in inverting Laplace transforms. The Riemann-sum approximation for the Laplace inversion involves a single summation for numerical process. Its accuracy depends on the value of ξ and the truncation error dictated by *N*. The value of ε must be selected so that the Bromwich contour encloses all the branch points [18]. For faster convergence, however, numerous numerical experiments have shown that a value satisfying the relation $\xi\eta$ $\xi\eta = 4.7$ gives the most satisfactory results (Vernotte 1961). Hence, the appropriate value of ξ for faster convergence depends on the instant of time (η) at which the lagging phenomenon is studied. The criterion shown by $\xi\eta = 4.7$ is independent of the value of η. The number *N* of terms used in the Riemann-sum is determined so that a prescribed threshold for the accumulated partial sum is satisfied at a given values of ξ, *Y*, and η.

III. Results And Discussion

Figure 2 shows the effect of *K*n on the velocity spatial distribution. As *K*n increases, the velocity slip at the wall increases which reduces the retarding effect of the wall. This yields an observable increase in the gas velocity near the wall. However, as *K*n increases, the temperature jump increases and this reduces the amount of heat transfer from the wall to the fluid. This reduction in heat transfer reduces the buoyancy effect, which derives the flow and hence reduces the gas velocity far from the wall. The reduction in velocity due to the reduction in heat transfer is offset by the increase in *U* due to the reduction in the frictional retarding forces near the wall.

The effect of D_a on the velocity spatial distribution is shown in Fig. 3. It is clear that small D_a numbers, less than 10^{-3}, have insignificant effect on the velocity slip at the wall of the microchannel. The effect of D_a numbers on the microchannel slip velocity becomes more significant as D_a increases. For D_a<10^{-3}, the frictional drag resistance against free convection is very large due to the small permeability of the porous domain and as a result, the velocity slip is very small.

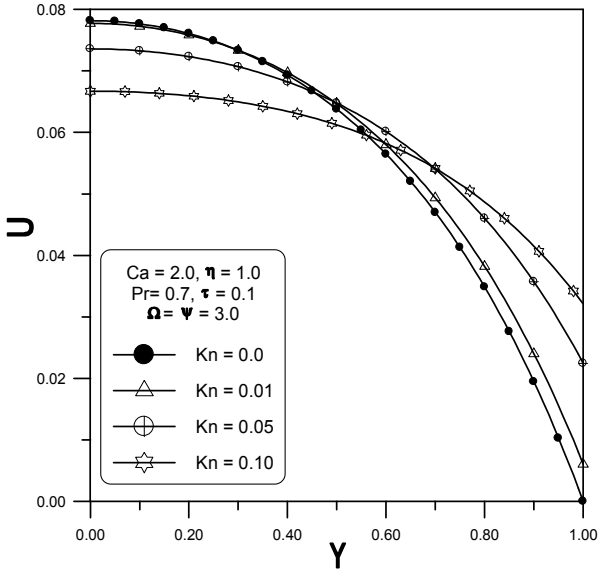

Fig. 2 Spatial velocity distribution at different Kn

Figure 4 shows the effect of *K*n on the spatial temperature distribution. As shown from this figure, increasing *K*n yields an increase in the temperature jump at the heated wall. This is

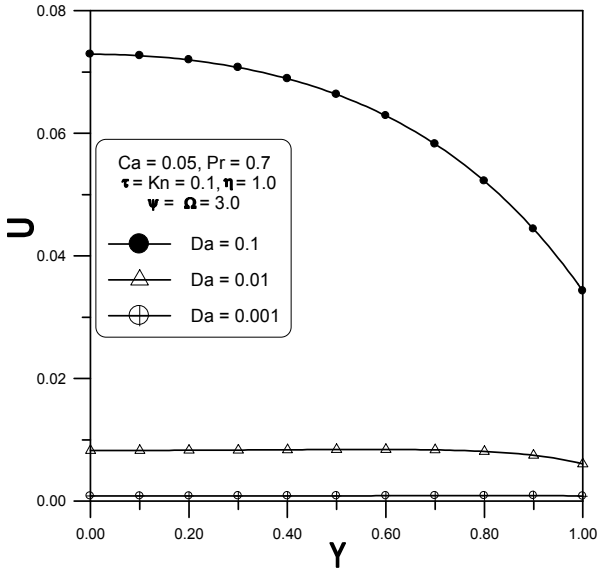

Fig. 3 Spatial velocity distribution at different Da

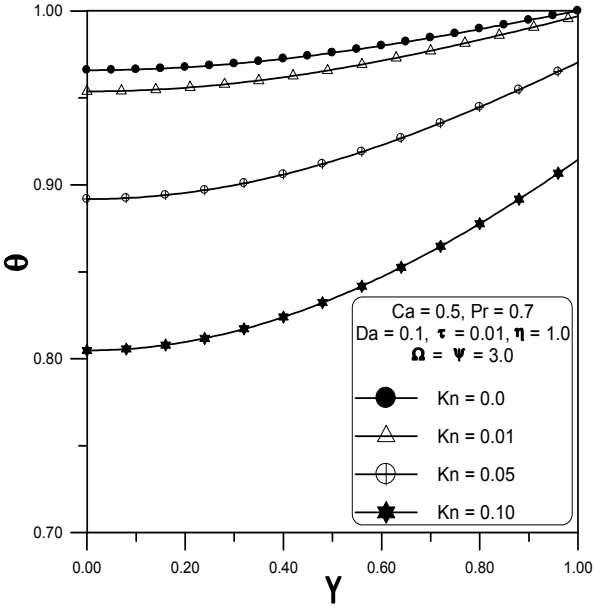

Fig. 4 Spatial temperature distribution at different Kn

due to the reduction in the interaction between the gas molecules and the heated wall. As *K*n number increases, the mean free path length of the gas molecules increases which implies that any molecule reflected from the wall has less opportunity to collide with other molecules and then to transmit it to the wall heating effect. Larger *K*n implies fewer molecules collide with the wall and carry part of its heating effect. As a result of increasing the temperature jump at the wall, less heat is transmitted to the gas, which yields less buoyancy driving force. This produces low temperature profiles at higher *K*n as clear from Fig. 4. The effect of the thermal relaxation time on the temperature spatial distribution is shown in Fig. 5. Increasing the thermal relaxation time τ yields an increase in the gas temperature especially in location far away from the heated wall.

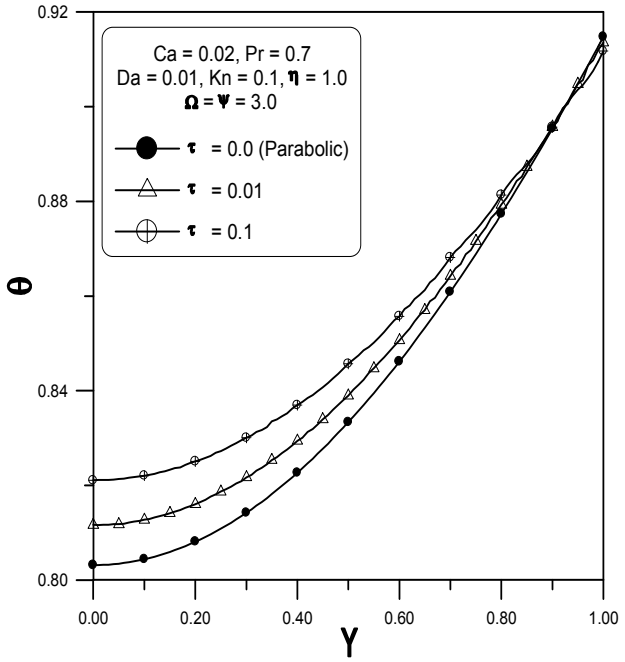

Fig. 5 Spatial temperature distribution at different τ

Increasing τ implies that the temperature response (the effect) precedes the heat flux (the cause). As a result, any increase in τ yields an increase in the temperature distribution at the same time. The effect of *K*n on the transient behavior of the wall temperature jump is shown in Fig. 6. It is clear that the temperature jump increases as *K*n increase as explained previously.

Also, it is clear that the temperature jump decreases as time proceeds and then approaches a very small, but nonzero, asymptotes especially at large values of *K*n.

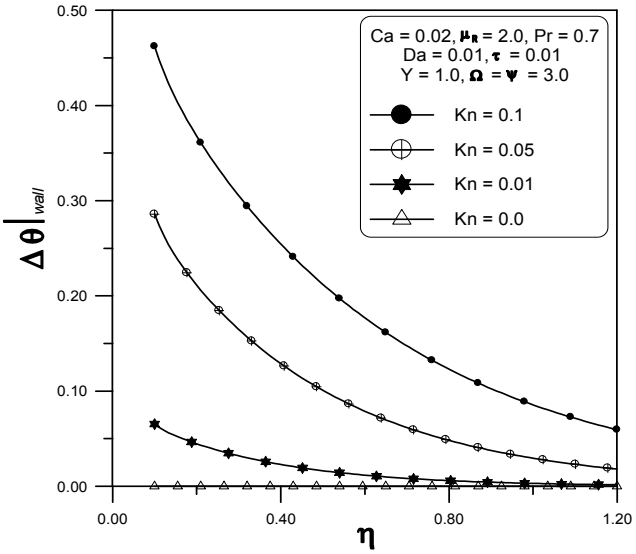

Fig. 6 Effect of Kn on the transient temperature difference at the wall

As time proceeds, the heating effect of the wall raises the gas temperature and the difference between the wall and the adjacent gas temperatures decreases.The effect of τ on the transient behavior of the wall temperature jump is shown in Fig. 7. It is clear that the temperature jump decreases as time proceeds as explained previously. The effect of τ is significant within the early stages of time.

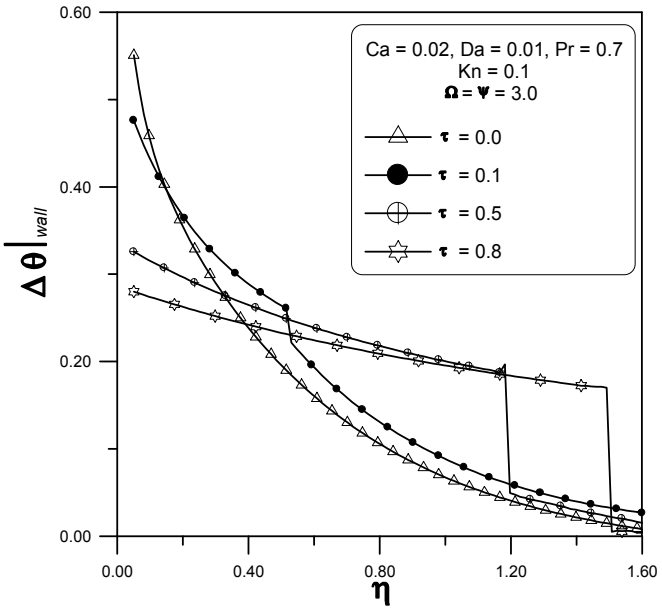

Fig. 7 Effect of τ on the transient temperature difference at the wall.

IV. Conclusion

The transient hydrodynamics and thermal behaviors of fluid flow in open-ended vertical parallel-plate microchannel filled with porous media are investigated semi-analytically under the effect of the hyperbolic heat conduction model. Microchannel hydrodynamics and thermal behaviors are affected by different parameters Kn , Kn D_a and τ. It is found that as Kn increases the slip in the hydrodynamic and thermal boundary condition increases. This slip in the hydrodynamic boundary condition increases as D_a increases. Also, the slip in the thermal boundary condition increases as τ decreases especially the early stage of time.

References

[1] Gad-el-Hak, Mohamed, *MEMs Introduction and Fundamentals,* 2ed ed. Taylor and Frances Group, LLC, 2006, ch. 4.
[2] G. Karniadakis, M. Beskok*, Micro flows fundamentals and simulation*. New York: Springer 2002.
[3] Y. Zohar, Heat convection in micro ducts. Kluwer 2003.
[4] Y. Zohar, W. Lee, S. Lee, L. Jiang, and P. Tong, "Subsonic gas flow in a straight and uniform microchannel," *J. Fluid Mech*. 472, pp. 125-151, 2002.
[5] C. Ho, Y. Tai, Micro-electro-mechanical systems (MEMS) and fluid flows. Ann. Rev. Fluid Mech. 30, 579612, 1998.
[6] M. A. Al-Nimr, and A. F. Khadrawi, Thermal behavior of a stagnant gas convicted in a horizontal microchannel as described by the dual-phase-lag heat conduction model, Int. J. Thermophysics, Vol. 25, pp. 1953, 2004.
[7] A. F. Khadrawi, A. Othman and M. A. Al-Nimr, Transient free convection fluid flow in a vertical microchannel as described by the hyperbolic heat conduction model, Int. J. Thermophysics, Vol. 26, pp.905, 2005.
[8] O. M. Haddad, M. M. Abuzaid and M. A. Al-Nimr, Entropy generation due to laminar incompressible forced convection flow through parallel-plates microchannel, Entropy, Vol. 6(5), pp. 413-426, 2004.
[9] O. M. Haddad, M. A. Al-Nimr, and M. M. Abuzaid, The effect of frequency of fluctuating driving force on basic slip micro-flows, Acta Mechanica , Vol. 179, pp. 249-259, 2005.
[10] O. M. Haddad, M. M. Abuzaid, and M. A. Al-Nimr, Developing free convection gas flow in a vertical open-ended micro-channel filled with porous media, Numerical Heat Transfer, Part A, Vol. 48 (2005).
[11] O. M., Haddad, M. A. Al-Nimr, and Y. Taamneh, Hydrodynamic and thermal behavior of gas flow in micro channels filled with porous media, J. Porous Media, Vol. 9(5), pp. 403-414, 2006.
[12] O. M., Haddad, M. A. Al-Nimr, and M. M. Abuzaid, Effect of periodically oscillating driving force on basic microflows in porous media, Journal Porous Media, Vol. 9(7), pp. 695-707, 2006.
[13] O.M. Haddad, M. A. Al-Nimr, and J. Sh. Al-Omary, Forced convection of gaseous slip-flow in porous micro-channels under local thermal non-equilibrium conditions, Transport in Porous Media, Vol. 67(3), pp. 453-471, 2007.
[14] O.M. Haddad, M. A. Al-Nimr, and M. Sari, Forced convection gaseous slip flow in circular porous micro-channels, Transport in Porous Media, Vol. 70(2), pp. 167-179 , 2007.
[15] J. Al-Jarrah, A. F. Khadrawi, and M. A. Al-Nimr, Film condensation on a vertical micro-channel, Int. Communication in Heat and Mass Transfer, Vol. 35(9), pp. 1172-1176, 2008.
[16] [18] P. Wu, W. A. Little, Measurement of friction factors for the flow of gases in very fine channels used for microminiature Joule Thompson refrigerators. Cryogenics 23, 273277, 1983.
[17] S. B. Choi, R. F. Barron, R. O. Warrington, Fluid flow and heat transfer in microtubes. Micromech. Sensors Actuators Sys. 32, 123134 1991.
[18] J. C. Harley, Y. Huang, H. Bau, J. N. Zemel, Gas flows in micro-channels. J. Fluid Mech. 284, 257274, 1995.
[19] S. F. Choquette, M. Faghri, E. J. Kenyon, B. Sunden, Compressible fluid flow in micron-sized channels. Nat. Heat Transfer Conf. 5, 2532 1996.
[20] Z. Y. Guo, X. B. Wu, Compressibility effects on the gas flow and heat transfer in a microtube. Int. J. Heat Mass Transf. 40, 32513254 ,1997.
[21] S. Kiwan, and M. A. Al-Nimr, "Flow and Heat Transfer over a Stretched Micro-Surface", ASME J Heat Transfer, Vol. 131(6), 2009.
[22] M. A., Al-Nimr, A. M., Maqapleh, A. F. Khadrawi, and Ammourah S. A.: "Fully developed thermal behaviors for parallel flow microchannel heat exchanger", International Communications in Heat and Mass Transfer Vol. 36, pp 385–390, 2009.
[23] K. Bataineh, and M. A. Al-Nimr, 2-D "Navier–Stokes Simulations of Microscale Viscous Pump with Slip Flow", ASME Journal of Fluids Engineering, Vol. 131, Issue 5, 2009.
[24] G. P. Duncan, G. P. Peterson, Review of microscale heat transfer. Appl. Mech. Rev. 47(9), 397428, 1994.
[25] Y. Yorozu, M. Hirano, K. Oka, and Y. Tagawa, "Electron spectroscopy studies on magneto-optical media and plastic substrate interfaces(Translation Journals style)," *IEEE Transl. J. Magn.Jpn*., vol. 2, Aug. 1987, pp. 740–741 [*Dig. 9th Annu. Conf. Magnetics* Japan, p. 301, 1982.

Nomenclature

C	Specific heat, J·kg-1·K-1
Ca	Acceleration coefficient tensor.
D_a	Darcy number, λ/L^2
F	Laplace transformation of the dimensionless velocity
Kn	Knudsen number, λ/L
K	thermal conductivity, *W·m-1·K*-1
K	permeability of the porous media.
L	characteristic length, m
Pr	Prandtl number, ν/α
Q	conduction heat flux, W·m-2
q_o	reference conduction heat flux, $k\Delta T/L$
Q	dimensionless conduction heat flux, q_o/q
S	Laplacian domain

t	time, s
T	temperature, K
T_∞	ambient and initial temperature, K
T_w	wall temperature, K
V	Laplace transformation of the dimensionless heat flux
U	axial velocity, m/s
u_o	reference velocity, $L^2 g\beta\,(T_w - T_\infty)/\nu$
U	dimensionless velocity, u/u_o
W	Laplace transformation of the dimensionless temperature
Y	transverse coordinate, m

Greek symbols

α	thermal diffusivity, m2·s-1
ΔT	dimensionless temperature difference, $T_w - T_\infty$
η	dimensionless time, $\nu t/L^2$
ε	porosity
ξ	real part of the Bromwich contour that is used in inverting Lap. transforms
γ	specific heat ratio
λ	mean free path, m
ν	kinematic viscosity, $m^2 \cdot s^{-1}$
σ_T	thermal accommodation coefficient
σ_v	tangential-mom.- accommodation coefficient
θ	dimensionless temp., $(T - T_\infty)/(T_w - T_\infty)$
$\bar{\tau}_T$	phase-lag in temperature gradient, s
$\bar{\tau}_q$	phase-lag in heat flux vector, s
τ_T	dimensionless phase-lag in temperature gradient, $\bar{\tau}_T\,\alpha/L^2$
τ_q	dimensionless phase-lag in heat flux vector, $\bar{\tau}_q\,\alpha/L^2$
Y	dimensionless transverse coordinate, y/L